© 2017. Published by The Company of Biologists Ltd | Journal of Cell Science (2017) 130, 2329-2343 doi:10.1242/jcs.196147

RESEARCH ARTICLE

Loss of β-PIX inhibits focal adhesion disassembly and promotes keratinocyte motility via myosin light chain activation

Sho Hiroyasu, Gregory P. Stimac, Susan B. Hopkinson and Jonathan C. R. Jones*

ABSTRACT

During healing of the skin, the cytoskeleton of keratinocytes and their matrix adhesions, including focal adhesions (FAs), undergo reorganization. These changes are coordinated by small GTPases and their regulators, including the guanine nucleotide exchange factor β-PIX (also known as ARHGEF7). In fibroblasts, β-PIX activates small GTPases, thereby enhancing migration. In keratinocytes *in vitro*, β-PIX localizes to FAs. To study β-PIX functions, we generated β-PIX knockdown keratinocytes. During wound closure of β-PIX knockdown cell monolayers, disassembly of FAs is impaired, and their number and size are increased. In addition, in the β-PIX knockdown cells, phosphorylated myosin light chain (MLC; also known as MYL2) is present not only in the leading edge of cells at the wound front, but also in the cells following the front, while p21-activated kinase 2 (PAK2), a regulator of MLC kinase (MYLK), is mislocalized. Inhibition or depletion of MYLK restores FA distribution in β-PIX knockdown cells. Traction forces generated by β-PIX knockdown cells are increased relative to those in control cells, a result consistent with an unexpected enhancement in the migration of single β-PIX knockdown cells and monolayers of such cells. We propose that targeting β-PIX might be a means of promoting epithelialization of wounds *in vivo*.

KEY WORDS: Cell motility, Collective cell migration, Adhesion, Cytoskeleton, Traction force

INTRODUCTION

During development and wound healing of epithelial tissues, cell–matrix adhesions and the cytoskeleton cooperatively function to regulate the traction forces of the cells on their substrate (Oakes and Gardel, 2014). These traction forces are needed for individual as well as groups of cells to migrate over the wound bed. Specifically, when a cell moves forward, the actin cytoskeleton protrudes at the leading edge and attaches to immature matrix adhesion sites enriched in focal adhesion (FA) proteins (sometimes termed focal complexes), which are located at the substratum-attached surface of the cell (Burnette et al., 2011). Actomyosin contraction causes slippage of FAs along the cell membrane, with each FA binding to elements of the extracellular matrix (Gallegos et al., 2011). The matrix-anchored FA is pulled by the actin cytoskeleton and transmits contraction forces to the substrate to generate the traction needed to move the cell forward. At the same time, conformational changes induced in certain FA proteins reveal binding sites for additional proteins, resulting in FA maturation (Gallegos et al., 2011). Indeed, some workers have likened this process to a ratchet with the actin cytoskeleton as the 'lever' and FAs functioning as the 'teeth' (Burnette et al., 2011).

In fibroblasts, astrocytes and certain epithelial cells, a protein termed β-PIX, a p21-activated kinase (PAK)-interacting guanine-nucleotide exchange factor (GEF) (also known as ARHGEF7 or COOL), is reported to be a negative regulator of FA maturation and is known to control FA size (Kuo et al., 2011; Zhao and Guan, 2011). β-PIX interacts with the PDZ domains of the tumor suppressor protein called Scrib and with paxillin, a FA component, via a protein termed G-protein-coupled receptor kinase-interacting target (GIT1 and GIT2) (Turner et al., 1999; Audebert et al., 2004). As a GEF, β-PIX activates the small GTPases Rac1 and Rho. Fibroblasts deficient in β-PIX move slower and exhibit a defect in directed migration since β-PIX is required to localize Rac1 to the front of a moving cell (Cau and Hall, 2005; ten Klooster et al., 2006). Moreover, β-PIX deficiency reduces the speed of lung epithelial cells and their directional persistence while chemotactic migration of β-PIX deficient breast epithelial cells is impaired (Audebert et al., 2004; Nola et al., 2008; Yu et al., 2015). Collective migration of anterior visceral endoderm cells is disrupted following deletion of β-PIX in mice (Omelchenko et al., 2014). Interestingly, notwithstanding β-PIX being a GEF, its reduction in both lung epithelial and anterior visceral endoderm cells results in either no change or an increase in Rac activity (Omelchenko et al., 2014; Yu et al., 2015). However, at least with regard to β-PIX knockout anterior visceral endoderm cells, Rac1 is mislocalized within the knockout cells, leading to the cells having multiple protrusions while lacking front–rear polarity (Omelchenko et al., 2014).

In the current study, our goal was to assess the role of β-PIX in the motility of single keratinocytes and groups of keratinocytes undergoing collective cell migration. Our data indicate that β-PIX deficient keratinocytes exhibit defects in FA disassembly compared to controls although they show no change in activation of Rac1. Surprisingly, both β-PIX-deficient single cells and wounded monolayers of keratinocytes migrate faster than control cells. Consistent with an increase in their speed, the traction forces generated by β-PIX-deficient cells are enhanced. Furthermore, we demonstrate that loss of β-PIX in keratinocytes results in an alteration in the distribution of activated myosin light chain (MLC, also known as MYL2) and a regulator of MLC kinase (MYLK), p21-activated kinase 2 (PAK2). We propose a model in which increased epidermal speed and a more efficient epithelialization of *in vitro* wounds is a result of this MLC activation, consequent actomyosin contraction and an increase in the traction forces exerted by the cells on their substrate.

RESULTS

β-PIX localizes to FAs at the leading edge of keratinocytes

We focused our initial analyses on determining the location of FA proteins, actin and β-PIX in scratch-wounded cultures of wild-type

School of Molecular Biosciences, Washington State University, Pullman, WA 99164, USA.

*Author for correspondence (jcr.jones@vetmed.wsu.edu)

S.H., 0000-0002-7696-2391; G.P.S., 0000-0001-8896-8945; S.B.H., 0000-0001-8647-5725; J.C.R.J., 0000-0002-1496-4922

Received 1 August 2016; Accepted 30 May 2017

Journal of Cell Science (2017) 130, 2329-2343 doi:10.1242/jcs.196147

HaCaT cells, particularly the leader cells moving over a wound *in vitro* and follower cells located within three to four cell layers immediately distal from the leaders of the group. Talin-1 (hereafter referred to as talin) and paxillin, both markers of FAs, mainly localize within 10 µm of the free edge of leader cells in small puncta (immature FAs, sometimes termed focal complexes) and variably sized FAs (Fig. 1A). There are no obvious differences in staining observed with anti-talin and -paxillin antibodies in these cells (Fig. 1A). FAs are relatively rare both at the rear of the leader cells and in follower cells although there are occasional groups of FAs away from cell edges (Fig. 1A). The overall FA organization in HaCaT cells we describe is consistent with observations by others (Stehbens et al., 2014). We quantified FA staining in our images and compared FA density within a zone, 10 µm thick, of the free surface of leader cells (leading front, LF) as well as FA density within a zone of ∼120 µm thickness, distal to the LF (for convenience we term this the distal zone, DZ). The DZ consists of both the rears of leader cells and several (up to four) layers of follower cells (Fig. 1A). There is a significant decrease in FA density in the DZ compared with the density in the LF (Fig. 1A,B). It should be noted that talin, paxillin and F-actin distribution in the DZ are similar, if not identical, to that in keratinocytes in intact monolayers (Fig. S1A).

β-PIX colocalizes with talin in FAs in both the LF and in the DZ (Fig. 1C). In some FAs in the LF of a wounded monolayer, β-PIX

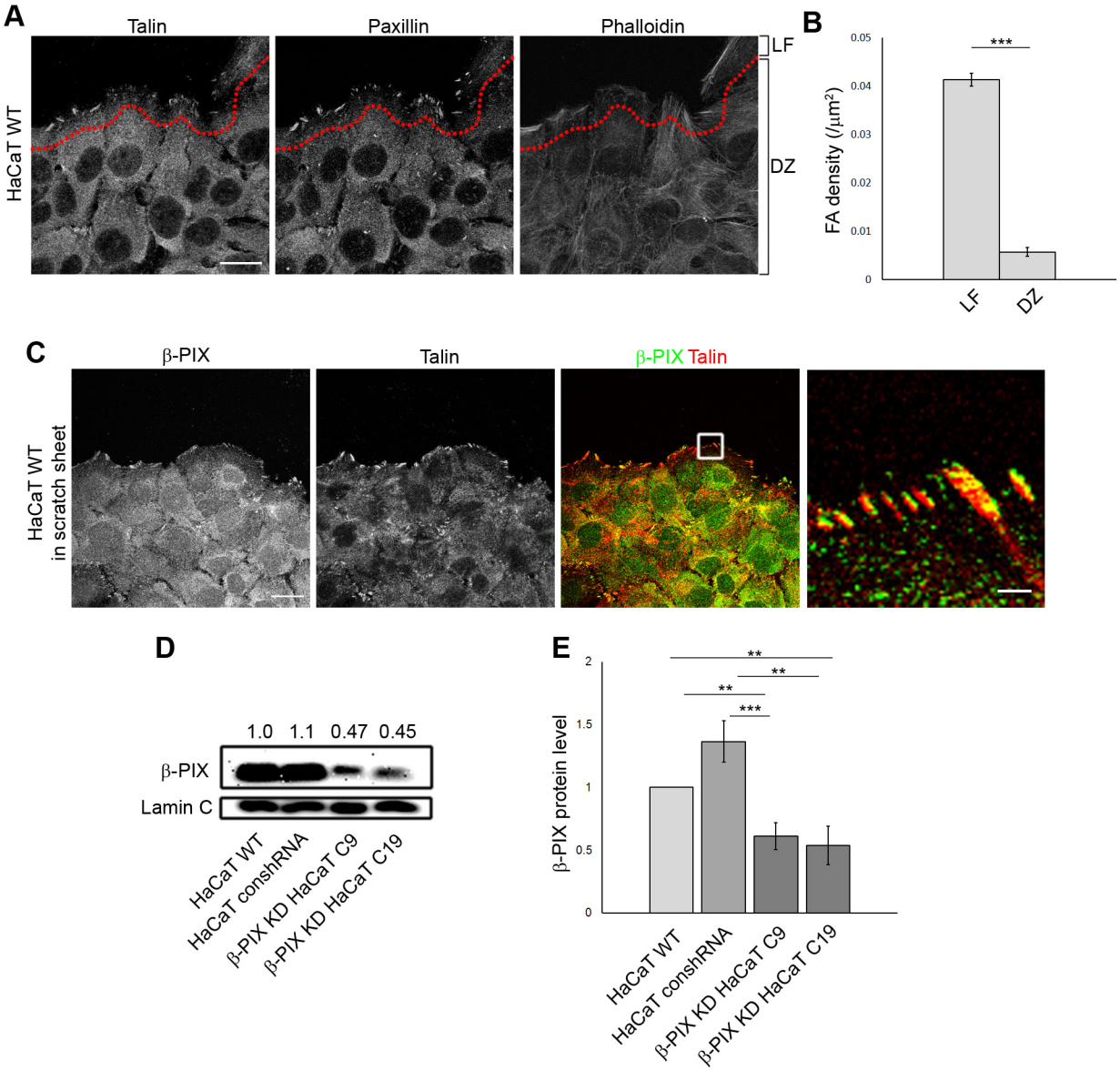

Fig. 1. FA protein localization in HaCaT cells. (A) Talin, paxillin and F-actin (labeled with phalloidin as indicated) localization in a scratch-wounded monolayer cell sheet of HaCaT cells at 4 h after wounding. The red dotted line indicates an arbitrary border between the leading front (LF) and distal zone (DZ) of the wounded monolayer (bracketed at the right of the images). Scale bar: 20 µm. (B) FA density at the LF and DZ in scratch-wounded monolayers of HaCaT cells as in A (mean±s.e.m.; *n*=4). (C) β-PIX and talin localization in a scratch-wounded monolayer at 4 h after wounding. The third panel from the left shows overlays of the two stains (green, β-PIX; red, talin). The boxed area is shown at a higher magnification in the fourth panel. Scale bars: 20 µm (first panel); 2 µm (fourth panel). (D) Extracts of parental HaCaT cells (HaCaT WT), HaCaT cells expressing control shRNA (HaCaT conshRNA), and two cloned lines of HaCaT cells expressing β-PIX shRNA (β-PIX KD HaCaT C9 and C19) were processed for immunoblotting using antibodies against β-PIX. Reactivity of a lamin antibody with lamin C was used as a loading control. (E) Immunoblots as in D were quantified and the levels of β-PIX protein normalized to the lamin C protein level in extracts are presented relative to those in HaCaT WT cells (set at 1) (means±s.e.m.; *n*=3 independent samples). ***P*<0.01, ****P*<0.001 (Student's *t*-test).

Journal of Cell Science (2017) 130, 2329-2343 doi:10.1242/jcs.196147

and talin staining in individual FAs does not completely overlap (Fig. 1C). In addition to its FA association, β-PIX can be seen distributed as small puncta throughout the cytoplasm of both leader and follower cells. These puncta are most obvious in the high-power image shown in Fig. 1C. Likewise, in intact cell sheets, β-PIX localizes to small puncta but is also co-distributed with talin in small FA-like structures (Fig. S1B). In single cells, β-PIX associates with talin-positive FAs, but the staining generated by talin and β-PIX antibodies does not necessarily overlap within individual FAs (Fig. S1C). β-PIX also localizes to small cytoplasmic puncta (Fig. S1C). In both single HaCaT cells and HaCaT cell sheets, β-PIX does not co-distribute with the hemidesmosome protein β4 integrin, which is found in puncta distinct from both FAs and the puncta stained by anti-talin and -paxillin antibodies (Fig. S1D; localizations of β-PIX and β4 integrin is only shown for cell sheets).

β-PIX KD HaCaT cells show increased single cell and collective cell motility

Localization of β-PIX to FAs has been reported to be accompanied by increased speed and processivity of lung epithelial cells (Yu et al., 2015). Moreover, its presence along the leading edge of keratinocytes covering wounds suggested to us that it might play a positive role in regulating wound closure. To test this possibility, we established cloned populations of HaCaT cells expressing β-PIX shRNA or control shRNA. In two KD clones expressing β-PIX shRNA (clones 9 and 19, respectively), we found 40 and 50% knockdown (KD) in β-PIX protein levels as determined by immunoblotting (Fig. 1D,E). Surprisingly, rather than reducing the speed of individual HaCaT cells, β-PIX KD resulted in an increase in the speed of single cells for the two KD clones on cell culture dishes and stiff gel substrates (Fig. 2A; Fig. S2A). Interestingly, on soft gel substrates the KD and control HaCaT cells move at the same speed, implying that β-PIX may be responsible for regulating speed by indirectly modulating the response of cell to the stiffness of its substrate (Fig. S2A). On the other hand, the processivity of single β-PIX KD cells is decreased when compared with their control counterparts on a stiff (cell culture dish) substrate (Fig. 2B). Moreover, collective cell migration of the two β-PIX KD HaCaT cell clones following scratch wounding is also enhanced compared to control cells both at 6 and 12 h after wounding (Fig. 2C).

FA size and localization in β-PIX KD HaCaT cells

Since the loss of β-PIX enhances the speed of HaCaT cells in both single cell and collective cell migration assays, we wondered what impact such deficiency has on keratinocyte FAs, the engine of their migration (Hopkinson et al., 2014). Antibodies against talin and paxillin show identical staining patterns in scratch-wounded monolayers of β-PIX KD HaCaT cells to control cells (Fig. 2D). However, compared to control cells, the size, density and distribution of FAs in β-PIX KD cells are all dramatically and significantly changed (Fig. 2D–F). Specifically, FAs are larger and more densely distributed, especially in the DZ regions of KD versus control cells (Fig. 2E,F). This is not simply a consequence of wounding since we also noted that FAs are more obvious in intact sheets of β-PIX KD HaCaT cells (Fig. S2B). Nonetheless, the ratio of staining intensities of vinculin to paxillin antibody and that of paxillin to talin antibody, respectively, at the site of each FA are not significantly different in control versus KD cells (Fig. S2C,D). However, actin stress fibers are more prominent in intact and wound-healing β-PIX KD HaCaT cells, particularly within the DZ (Fig. 2D; Fig. S2B). This change in cytoskeleton organization following β-PIX KD is consistent with reports using other cell types (Yu et al., 2015).

As is the case in cell sheets, in single β-PIX KD cells, FAs stained by anti-paxillin antibodies are larger than in parental cells (Fig. S2E). They also localize around the entire cell edge, rather than showing the polarized distribution typically observed in their control counterparts (Fig. S2E). Likewise, the hemidesmosome protein β4 integrin, which primarily localizes to the leading front of control cells, localizes along the entire edge of KD cells (Fig. S2E). In addition, actin stress fibers are also more prominent in single β-PIX KD cells (Fig. S2E).

β-PIX KD N/TERT cells show increased motility and changes in FA and cytoskeleton organization

To rule out that the motility and FA changes we observe in β-PIX KD keratinocytes is a peculiarity of HaCaT cells, we generated populations of another immortalized human keratinocyte cell line, specifically N/TERT cells, with deficiency in β-PIX protein (Dickson et al., 2000). The two N/TERT KD clones (clone 2 and 3) exhibit a decrease of 70 and 75% in the levels of β-PIX protein, respectively, relative to control cells (Fig. 3A,B). Both clones show enhanced motility in collective cell migration (Fig. 3C). FAs in control N/TERT cells are more prominent within the LF region compared with those in the DZ (Fig. 3D–F). In both KD clones, FAs are larger and denser, especially in the DZ (Fig. 3D–F). Moreover, actin stress fibers are more conspicuous in β-PIX KD N/TERT cells (Fig. 3D).

Expression of GFP-tagged β-PIX restores motility, FA size and FA localization in β-PIX KD HaCaT cells

To confirm that infection and/or expression of β-PIX shRNA have no off-target effects in keratinocytes, we transfected β-PIX KD HaCaT cells with mRNA encoding green fluorescent protein (GFP)-tagged β-PIX that is refractory to the β-PIX shRNA used to deplete the cells of endogenous β-PIX message (only results using clone 9 are shown in this and subsequent experiments). After transfection, cells were processed for fluorescence-activated cell sorting (FACS) and a relatively uniform population of GFP-positive cells, expressing ∼1.7-fold the level of endogenous β-PIX protein as assayed by immunoblotting, was selected (β-PIX KD HaCaT+GFP β-PIX) (Fig. 4A,B; Fig. S3A,B). As a control, GFP-negative [GFP(−)] cells were also isolated from the same transfected population (Fig. 4B–D). We compared the motility of wild-type, β-PIX KD, GFP(−) and β-PIX KD HaCaT+GFP β-PIX cells. The speed and processivity of GFP–β-PIX-expressing KD cells are comparable to those of wild-type cells, whereas GFP(−) cells exhibit the motile behavior of their β-PIX KD parents (Fig. 4C,D). In addition, FAs in GFP–β-PIX-expressing KD cells are similar in size to that observed in wild-type HaCaT cells, while FAs in GFP(−) cells are comparable in size to that in β-PIX KD cells (Fig. 4E,F).

FA assembly and disassembly in β-PIX KD HaCaT cells

The large size and density of FAs in β-PIX KD cells suggested to us that loss of β-PIX might affect FA assembly and/or disassembly. To test this possibility, we monitored the dynamics of GFP-tagged paxillin as a marker of FAs in live control and β-PIX KD HaCaT cells. FAs are more persistent in β-PIX KD HaCaT cells than those in control cells (Fig. 5A). Moreover, FAs in β-PIX KD cells exhibit a FA disassembly defect in both the LF and DZ, although FA assembly is not significantly changed (Fig. 5B,C).

Journal of Cell Science (2017) 130, 2329-2343 doi:10.1242/jcs.196147

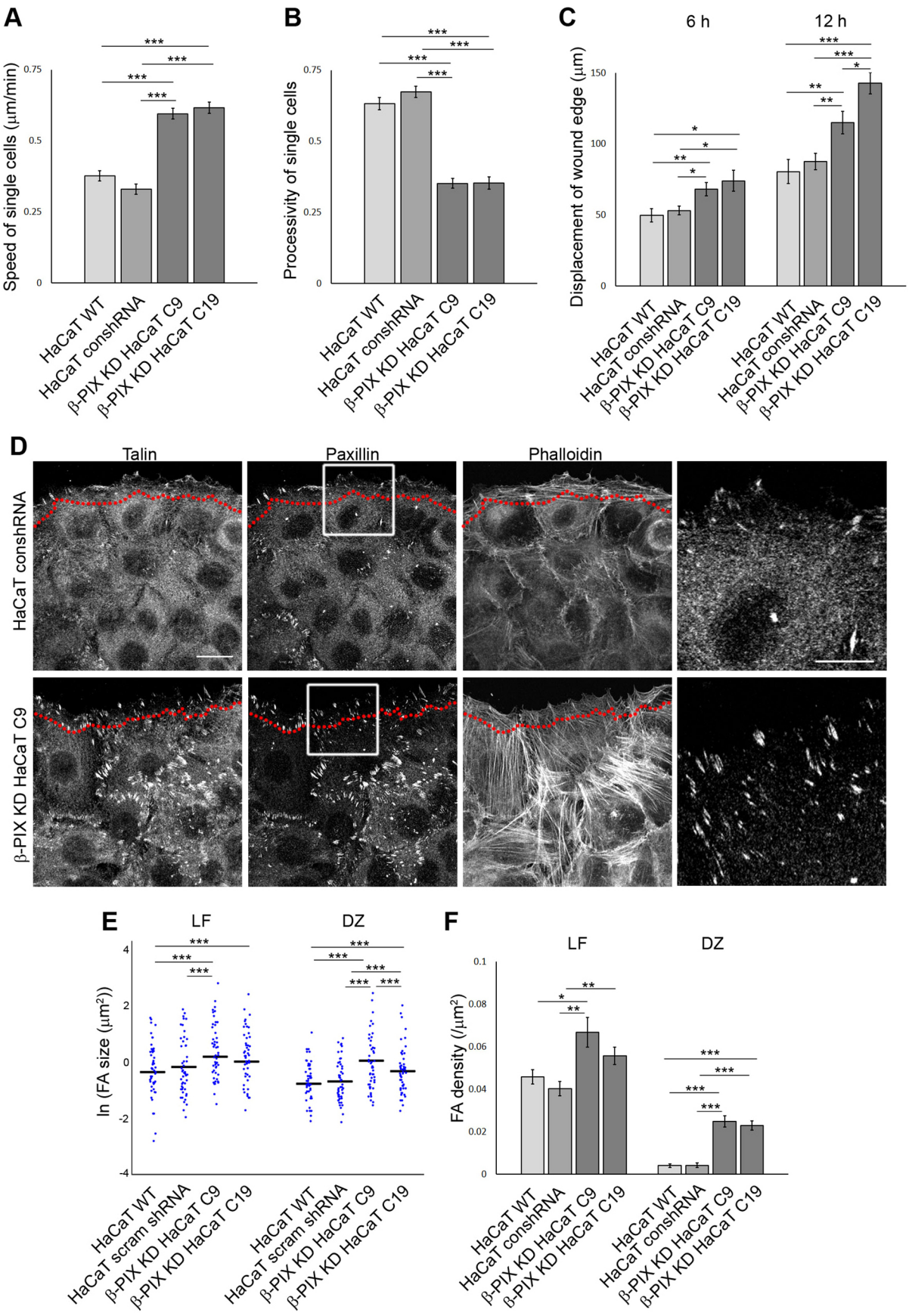

Fig. 2. See next page for legend.

Journal of Cell Science (2017) 130, 2329-2343 doi:10.1242/jcs.196147

Fig. 2. Motility, FA size and FA density changes in β-PIX KD HaCaT cells. Migration speed (A) and processivity (B) of single parental HaCaT cells (HaCaT WT), HaCaT cells expressing control shRNA (HaCaT conshRNA), and β-PIX KD HaCaT C9 and C19 cells (n=74 cells each). (C) Quantification of the displacement of the wound edge at 6 and 12 h after scratching of the indicated monolayers (n=3 independent assays with a minimum of four measurements per wound). (D) Localization of talin, paxillin and F-actin (phalloidin) in a scratch-wounded monolayer cell sheets of HaCaT cells expressing conshRNA and β-PIX KD HaCaT cells at 4 h after wounding. The red dotted line demarcates the border of the LF and DZ as in Fig. 1A. Boxed areas in the second panels from the left are shown at a higher magnification in the fourth panels. Scale bars: 20 µm (first panel); 10 µm (fourth panel). (E) The logarithmic transformation of FA sizes in the LF and DZ of HaCaT WT (n=187 in LF, n=233 in DZ), HaCaT conshRNA (n=144 in LF, n=139 in DZ), β-PIX KD HaCaT C9 (n=279 in LF, n=1066 in DZ), and β-PIX KD HaCaT C19 (n=151 in LF, n=716 in DZ) cells are presented graphically; 40 randomly selected FA sizes are shown in each case but the means (horizontal bars) are of all FAs assayed. (F) FA density in the LF and DZ of HaCaT WT, HaCaT conshRNA, β-PIX KD HaCaT C9 and β-PIX KD HaCaT C19 cells. FAs in a minimum of 12 areas were assayed in three independent studies in E and F. All bar graphs show means±s.e.m. *P<0.05, **P<0.01, ***P<0.001 (Student's t-test).

β-PIX-induced PAK2 recruitment in FAs is important for cell motility and FA organization in HaCaT cells

Consistent with work on other cell types, we observe no difference in Rac1 activity in β-PIX KD HaCaT cells compared to that in control cells (Fig. 6A) (Nola et al., 2008). β-PIX is also known to regulate the recruitment of the PAK family of serine/threonine p21-activated kinases to FA through its SH3 domain (Zhao et al., 2000). Thus, we analyzed the level and localization of PAK2 in control and β-PIX KD HaCaT cells. We detect no difference in PAK2 protein levels in control versus β-PIX KD cells as assessed by immunoblotting (Fig. 6B). However, whereas PAK2 localizes to FAs in control HaCaT leader cells following wounding, it appears to be diffusely distributed in β-PIX KD cells under the same conditions (Fig. 6C). This suggested to us that a major function for β-PIX in keratinocytes might be to recruit PAK2 to FAs. To test this possibility, we transfected β-PIX KD HaCaT cells with mRNA encoding a β-PIX SH3 domain mutant (W43P and W44G) tagged with GFP (GFP SH3-mutant β-PIX). This β-PIX mutant does not bind PAK or Rac1 (Manser et al., 1998; ten Klooster et al., 2006). Moreover, we also induced the expression of a β-PIX GEF domain mutant (L238R and L239S) tagged with GFP (GFP GEF-deficient β-PIX) in β-PIX KD HaCaT cells. This mutant protein cannot activate small GTPases (Manser et al., 1998). In both instances, following transfection, cell populations were prepared for FACS and cells expressing tagged mutant proteins were selected on the basis of GFP signal to confirm that the levels of GFP-tagged proteins were comparable to that of the GFP-tagged wild-type protein expressed in β-PIX KD HaCaT cells (Fig. S3C,D). GFP SH3-mutant β-PIX does not restore the motility behavior of β-PIX KD cells nor FA size, emphasizing the important function of β-PIX in mediating recruitment of both PAK2 and Rac1 to FAs (Fig. 4C–F). In contrast, motile behavior and FA size are restored in β-PIX KD cells expressing the GEF-deficient β-PIX mutant (Fig. 4C–F). The latter result is consistent with the lack of effect of β-PIX deficiency on Rac1 activity in HaCaT cells (Fig. 6A).

Inhibition or depletion of MYLK restores motility and FA organization in β-PIX KD HaCaT cells

Since PAK has been reported to regulate the levels of phosphorylated MLC (pMLC), either positively or negatively (Chew et al., 1998; Sanders et al., 1999; Sells et al., 1999), we also analyzed protein levels and localization of pMLC in control and β-PIX KD HaCaT cells. Although pMLC protein levels are unchanged in KD cells, pMLC localizes not only at the free edges of the scratch-wounded cell sheet but also in follower cells along actin stress fibers, a localization rarely observed in control cells (Fig. 6D,E).

To assess whether the localization change of pMLC observed in β-PIX KD is responsible for the size and localization changes of FAs we observe in KD cells, the latter were treated with the myosin light chain kinase (MYLK) inhibitor ML-7 or MYLK siRNA. The effect of MYLK KD was confirmed by real-time quantitative PCR (RT-qPCR) (Fig. S4A). Following these treatments, FAs are primarily restricted to the LF in a manner similar to that observed in control cells (Fig. 7A,C). Following ML-7 treatment, we observe a decrease in FA size only in the LF, and following MYLK KD, we observe it only in the DZ (Fig. 7B). Consistent with the recovery of FA organization, ML-7 treatment also reduces collective cell motility of β-PIX KD HaCaT cells (Fig. 7D). To assess whether myosin II-dependent actomyosin contraction, which is the regulated by MYLK, also impacts upon FA organization in the β-PIX KD cells, we treated the KD cells with blebbistatin. There is a dramatic decrease in FA numbers in both the LF and DZ of treated KD cells (Fig. 7A). Indeed, the loss of FAs throughout the cultures made quantification of FA size and density impossible.

Since Rho-associated protein kinases (ROCK, both ROCK1 and ROCK2) also affects FA size and cell motility through phosphorylation of MLC, we treated β-PIX KD HaCaT cells with the ROCK inhibitor Y-27632. Following the treatment, FA size and density both decreased, with the exception of FA density in the LF (Fig. S4B–D). However, cell motility is enhanced in KD cells following a 6 h incubation with Y-27632, consistent with another study (Fig. S4E) (Jackson et al., 2011). Since Y-27632 appears to be toxic when cells are treated for 12 h, we could not analyze collective cell migration for 12 h following scratch wounding.

Traction force magnitude is increased in β-PIX KD HaCaT cells

The generation of traction forces by cells is essential for motility and requires cytoskeleton coupling to matrix adhesion sites (Oakes and Gardel, 2014). The impact of β-PIX KD on FAs, cytoskeleton organization and MLC activation led us to investigate whether these changes result in modulation of the traction forces exerted by cells on their substrate. To do so, we plated HaCaT cells onto a fluorescent bead-embedded gel substrate as described previously (Eisenberg et al., 2013; Hiroyasu et al., 2016). We then compared traction force localization and magnitudes exerted by a control cells, β-PIX KD HaCaT clones and GFP-tagged β-PIX expressing β-PIX KD HaCaT cells. Control cells have traction force foci along the cell edges, while KD cells tend to have traction force foci mainly at the cell edge, with a few traction forces clustered around the center of the cells (Fig. 8A). The total magnitude of traction forces exerted by β-PIX KD HaCaT cell on their substrate is significantly increased compared to that of control and GFP-tagged β-PIX expressing β-PIX KD HaCaT cells (Fig. 8B).

DISCUSSION

In many cell types, β-PIX localizes to the site of FAs through binding to the FA component paxillin (Turner et al., 1999). Similar to former reports of β-PIX knockout or knockdown cells, we demonstrate here that β-PIX-deficient keratinocyte possess FAs that are both larger and more persistent than their counterparts in wild-type cells (Yu et al., 2015). This is consistent with the notion that β-PIX in keratinocytes enhances FA disassembly via an impact on

Journal of Cell Science (2017) 130, 2329-2343 doi:10.1242/jcs.196147

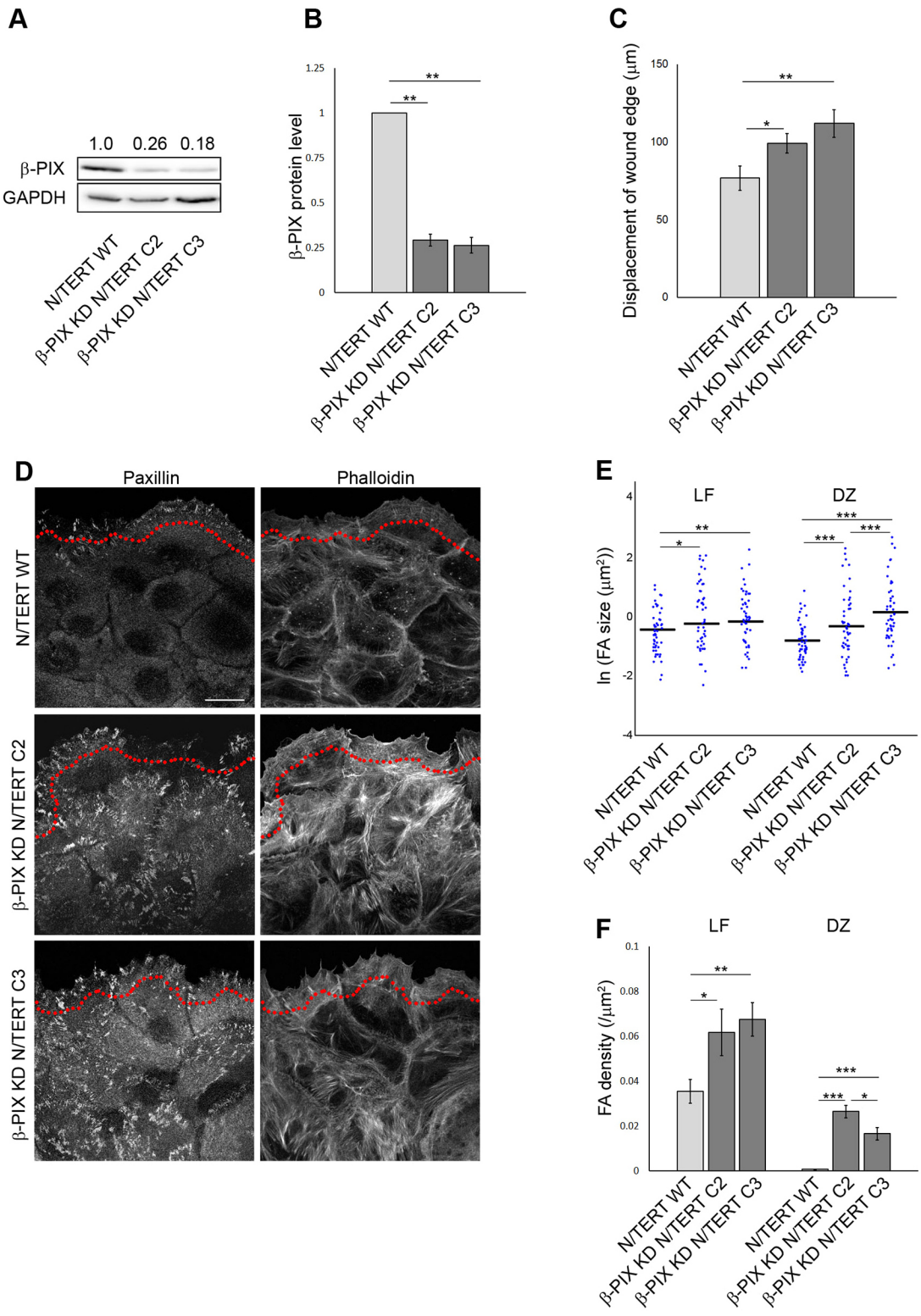

Fig. 3. Motility, FA size and FA density changes in β-PIX KD N/TERT cells. (A) Extracts of parental N/TERT cells (N/TERT WT) and two cloned lines of N/TERT cells expressing β-PIX shRNA (β-PIX KD N/TERT C2 and C3) were processed for immunoblotting using antibodies against β-PIX. Reactivity of an anti-GAPDH antibody was used as a loading control. (B) Immunoblots as in A were quantified and the levels of β-PIX protein in extracts, normalized to the GAPDH protein level, relative to those in N/TERT WT cells presented (n=3 independent samples). (C) Quantification of the displacement of the wound edge at 6 h after scratching of the indicated monolayers (n=3 independent assays with a minimum of four measurements per wound). (D) Localization of paxillin and F-actin (using phalloidin) in scratch-wounded monolayer cell sheets of N/TERT WT and β-PIX KD N/TERT cells at 4 h after wounding. The red dotted line demarcates the border of the LF and DZ as in Fig. 1A. Scale bar: 20 µm. (E) Logarithmic transformation of FA sizes in the LF and DZ of N/TERT WT (n=123 in LF, n=57 in DZ) and β-PIX KD N/TERT C2 (n=219 in LF, n=745 in DZ) and C3 (n=236 in LF, n=532 in DZ) cells is presented graphically; 40 randomly selected FA sizes are shown in each case but the means (horizontal bars) are of all FAs assayed. (F) FA density in the LF and DZ of N/TERT WT and β-PIX KD N/TERT cells. A minimum of eight areas were assayed in three independent studies in E and F. All bar graphs show means±s.e.m. *P<0.05, **P<0.01, ***P<0.001 (Student's t-test).

Journal of Cell Science (2017) 130, 2329-2343 doi:10.1242/jcs.196147

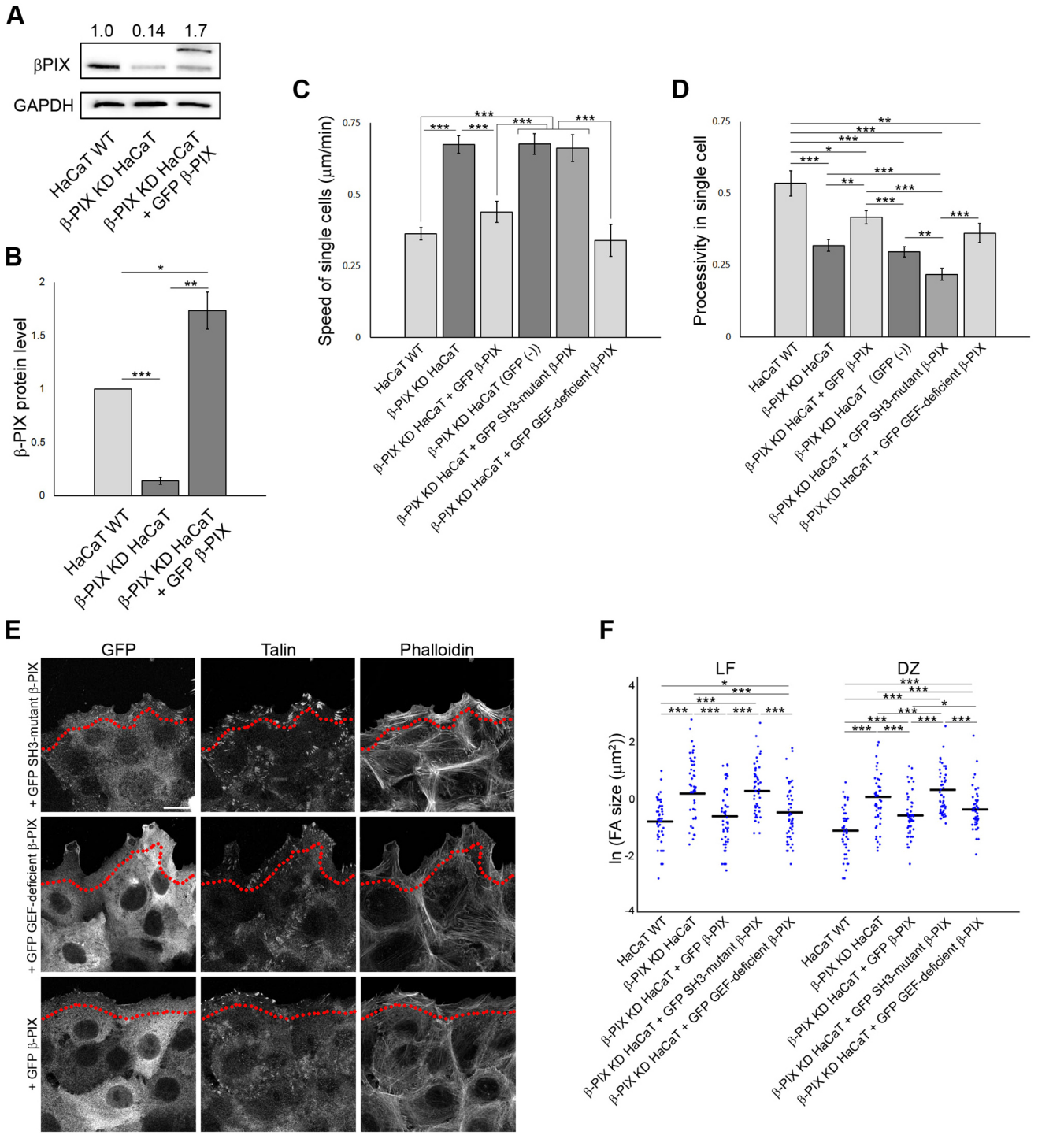

Fig. 4. GFP-tagged β-PIX restores FA size and density, and cell motility in β-PIX KD HaCaT cells. (A) Extracts of HaCaT WT, β-PIX KD HaCaT and β-PIX KD HaCaT cells transfected with GFP-tagged β-PIX followed by FACS-sorting according to GFP intensity (β-PIX KD HaCaT+GFP β-PIX) were processed for immunoblotting using antibodies against β-PIX. Reactivity of a GAPDH antibody was used as a loading control. (B) Immunoblots as in A were quantified and the levels of β-PIX protein in extracts, normalized to the GAPDH protein level, relative to those in HaCaT WT cells presented (*n*=3 independent samples). Quantification of speed (C) and processivity (D) of single cells in the populations of HaCaT WT cells, β-PIX KD HaCaT cells, β-PIX KD HaCaT+GFP β-PIX, β-PIX KD HaCaT cells transfected with GFP-tagged β-PIX followed by FACS and selected for their low level of GFP intensity [β-PIX KD HaCaT (GFP (−))], FACS-sorted β-PIX KD HaCaT cells expressing GFP-tagged SH3 mutant β-PIX (β-PIX KD HaCaT+GFP SH3-mutant β-PIX), and FACS-sorted β-PIX KD HaCaT cells expressing GFP-tagged GEF-deficient β-PIX (β-PIX KD HaCaT+GFP GEF-deficient β-PIX). A minimum of 25 cells in three independent studies were analyzed. (E) Localization of GFP, talin, and F-actin (phalloidin) in a scratch-wounded monolayer of β-PIX KD HaCaT+GFP SH3 mutant β-PIX, +GFP GEF-deficient β-PIX or +GFP β-PIX cells. The red dotted line demarcates the border of the LF and DZ as in Fig. 1A. Scale bar: 20 µm. (F) Logarithmic transformation of FA sizes in the LF and DZ of HaCaT WT (*n*=274 in LF, *n*=229 in DZ), β-PIX KD HaCaT (*n*=223 in LF, *n*=1066 in DZ), β-PIX KD HaCaT+GFP β-PIX (*n*=149 in LF, *n*=196 in DZ), β-PIX KD HaCaT+GFP SH3-mutant β-PIX (*n*=138 in LF, *n*=237 in DZ) and β-PIX KD HaCaT+GFP GEF-deficient β-PIX (*n*=138 in LF, *n*=172 in DZ) cells; 40 randomly selected FA sizes are shown in each case but the means (horizontal bars) are of all FAs assayed. A minimum of eight areas were assayed in three independent studies. All bar graphs show means±s.e.m. **P*<0.05, ***P*<0.01, ****P*<0.001 (Student's *t*-test).

Journal of Cell Science

Journal of Cell Science (2017) 130, 2329-2343 doi:10.1242/jcs.196147

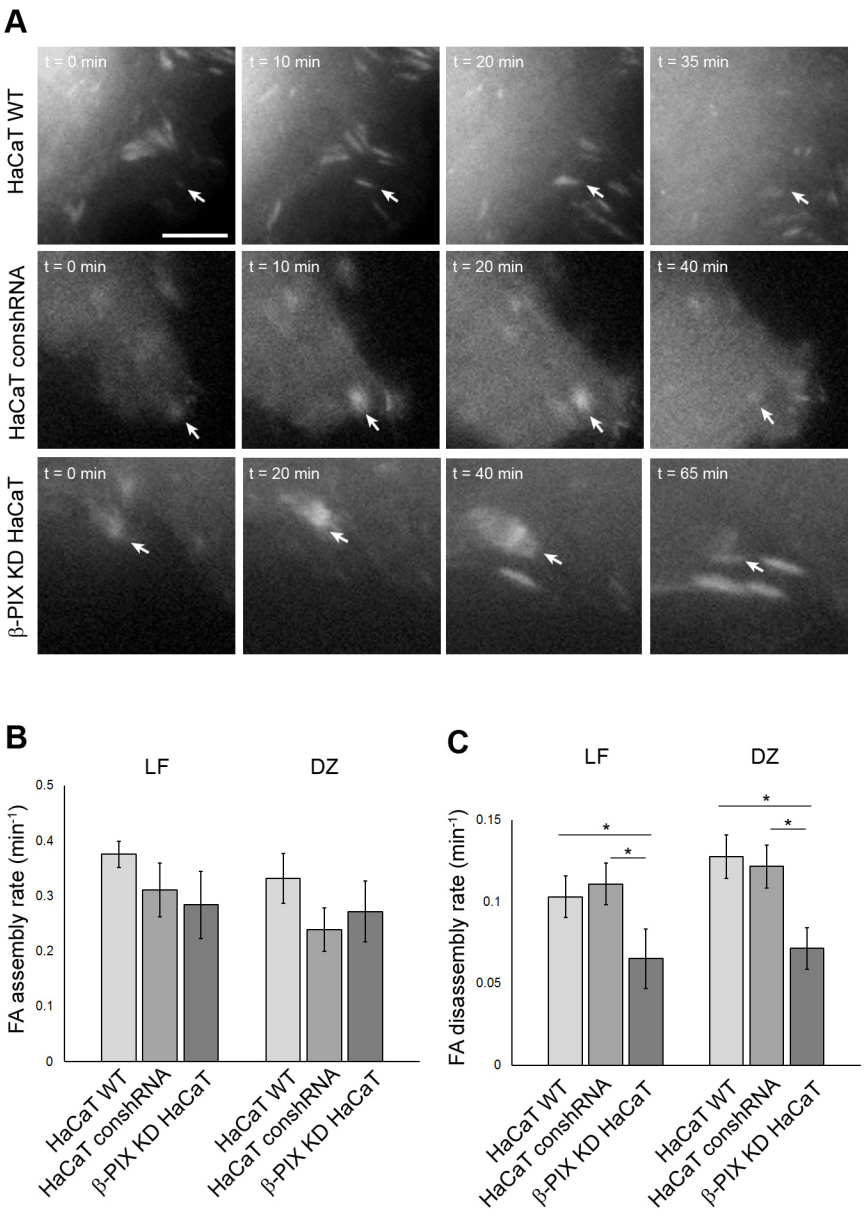

Fig. 5. FA assembly and disassembly in β-PIX KD HaCaT cells. (A) Still images of time-lapse imaging of GFP-tagged paxillin-expressing parental HaCaT cells (HaCaT WT), HaCaT cells expressing control shRNA (HaCaT conshRNA) and β-PIX KD HaCaT cells. FAs within the LF are shown. The first panels on the left (t=0 min) are the first frames in which the indicated FAs were observed, while the last panels on the right are the last frames in which the same FAs were visible. Scale bar: 5 µm. Quantification of FA assembly (B) and disassembly (C) rates of the indicated cells in both the LF and DZ. A minimum of eight FAs in three independent studies were analyzed. Values are means±s.e.m. **P*<0.05 (Student's *t*-test).

FA dynamics. Moreover, one of the consequences of β-PIX KD in keratinocytes is a loss of PAK2 from FAs. That PAK2 interaction with β-PIX is important in keratinocyte motility and for FA organization is supported by our finding that a GEF-deficient β-PIX, but not its SH3 mutant counterpart, is able to rescue both the motility defects and FA size changes we observe in β-PIX KD cells. Thus, we suggest that β-PIX deficiency and consequent loss of PAK2 from FAs likely changes FA functions and dynamics in keratinocytes, as is the case in axons (Santiago-Medina et al., 2013).

We also demonstrate that β-PIX KD results in an activation and redistribution of pMLC in keratinocytes. This may also be due to changes in PAK2 localization, since PAK family members directly regulate pMLC in several cell systems (Chew et al., 1998; Kiosses et al., 1999; Sanders et al., 1999; Sells et al., 1999; Goeckeler et al., 2000). Regardless, the importance of MLC in regulating FA size and localization in β-PIX KD keratinocytes is emphasized by the finding that the MLCK inhibitor ML-7 and MYLK KD restore FA localization and size in β-PIX KD keratinocytes, especially for follower cells, to that observed in wild-type cells. Taken together, these data suggest that in wild-type cells β-PIX promotes disassembly of FA via an ability to induce actomyosin relaxation, whereas its loss results in enhanced myosin-mediated actin cytoskeleton contraction leading to an inhibition in FA disassembly. This conclusion is supported by work from others who have shown that the actin cytoskeleton regulates FA disassembly through the regulation of actomyosin tension (Wolfenson et al., 2011).

In fibroblasts, astrocytes and certain epithelial cells, β-PIX functions to localize Rac1 and Cdc42 to the front of cells, and by doing so promotes actin filament-mediated extension of the leading lamellipodium and directed migration of a moving cell, rather than on the activation state of Rac1 per se (Audebert et al., 2004; Cau and Hall, 2005; Nola et al., 2008; Omelchenko et al., 2014). Our data also indicate that loss of β-PIX impedes processivity of keratinocytes, at least at the single-cell level, without impacting Rac1 activation levels. We assume that this is due to Rac1 mislocalization, as suggested by others (Omelchenko et al., 2014) (Fig. 8C,D). We have attempted to assess whether this is the case by

Journal of Cell Science (2017) 130, 2329-2343 doi:10.1242/jcs.196147

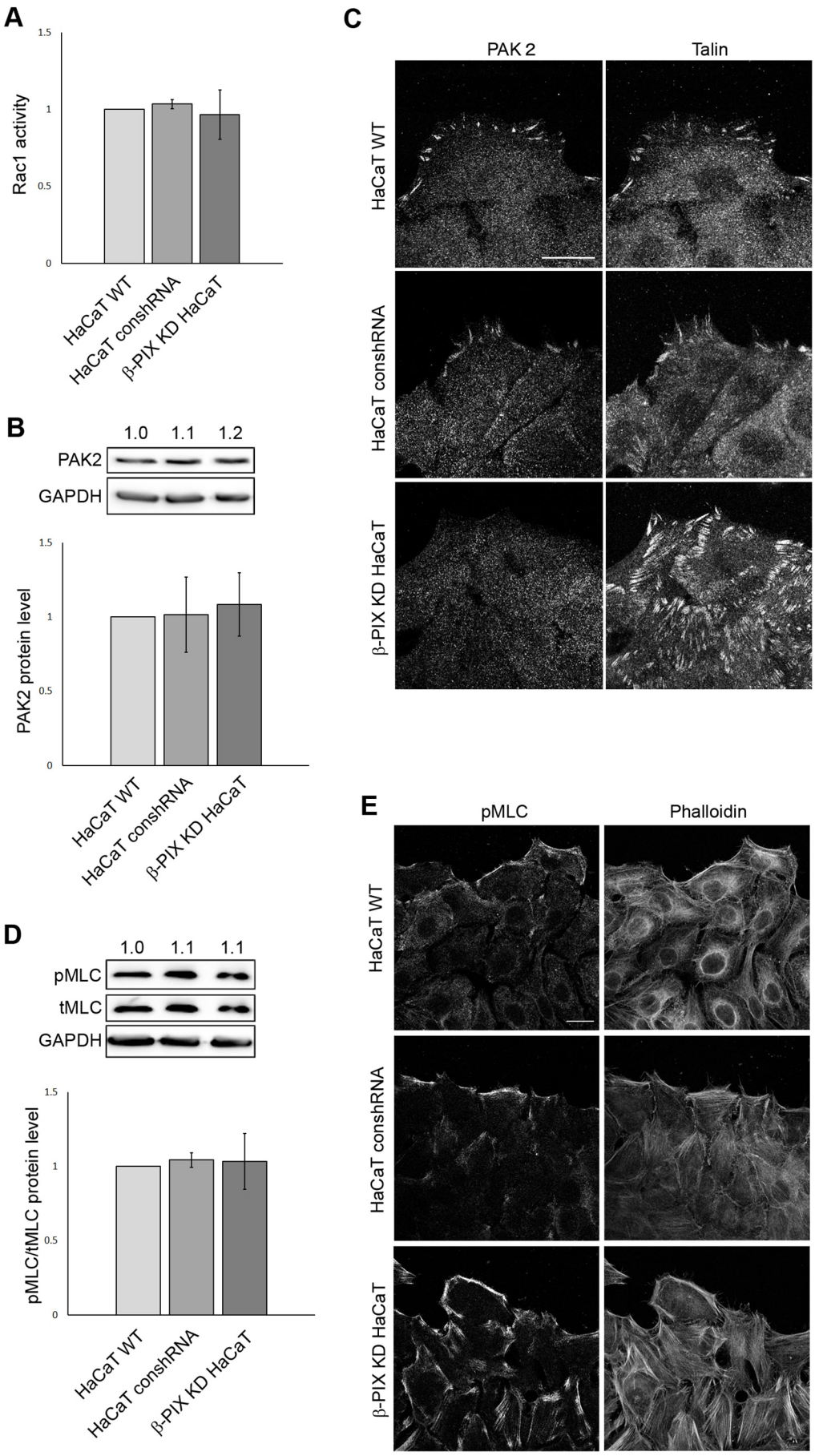

Fig. 6. PAK2 and pMLC protein levels and localization in β-PIX KD HaCaT cells. Rac1 activity (A) and levels of PAK2 (B) and pMLC (D) in extracts of a scratch-wounded monolayer of parental HaCaT cells (HaCaT WT), HaCaT cells expressing control shRNA (HaCaT conshRNA) and β-PIX KD HaCaT cells at 4 h post wounding (n=3). (A) Rac1 activity was evaluated using a G-LISA. (B,D) PAK2, pMLC and total MLC levels were assayed by immunoblotting. GAPDH and total MLC reactivities were used as loading controls. Values are means±s.e.m. No significant differences are detected in A, B and D (Student's t-test). Localization of PAK2 and talin (C), or pMLC and F-actin (phalloidin) (E) in the indicated scratch-wounded monolayer cell sheets at 4 h post wounding. Scale bars: 20 µm.

Journal of Cell Science (2017) 130, 2329-2343 doi:10.1242/jcs.196147

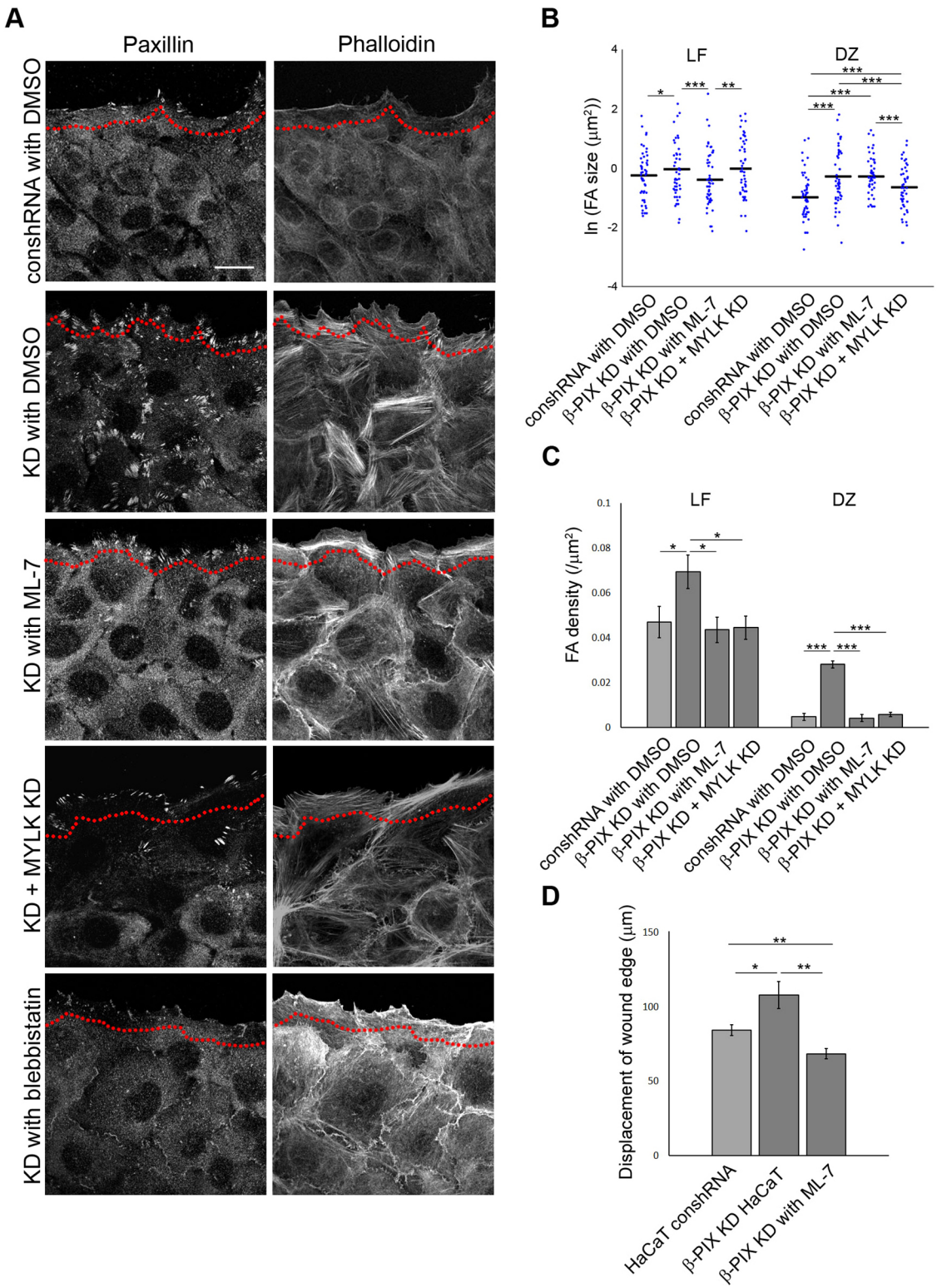

Fig. 7. Inhibition or depletion of MYLK restores FA localization and motility in β-PIX KD HaCaT cells. (A) Paxillin and F-actin (phalloidin) localization in a scratch-wounded monolayer cell sheet of HaCaT cells expressing control shRNA (HaCaT conshRNA) and β-PIX KD HaCaT cells incubated with either DMSO, ML-7 or blebbistatin, as indicated. The panels indicated as KD+MYLK KD show staining in a scratch-wounded monolayer sheet of β-PIX KD HaCaT cells expressing siRNA targeting MYLK. The red dotted lines mark the arbitrary border of the LF and DZ as in Fig. 1A. Scale bar: 20 µm. (B) Logarithmic transformation of FA sizes in the LF and DZ of DMSO-treated HaCaT conshRNA (*n*=143 in LF, *n*=119 in DZ), DMSO-treated β-PIX KD HaCaT (*n*=253 in LF, *n*=892 in DZ), ML-7-treated β-PIX KD HaCaT (*n*=130 in LF, *n*=90 in DZ), and MYLK siRNA-expressing β-PIX KD HaCaT (*n*=82 in LF, *n*=118 in DZ) cells; 40 randomly selected FA sizes are shown in each case but the means (horizontal bars) are of all FAs assayed. (C) FA density in the LF and DZ of DMSO-treated HaCaT conshRNA, DMSO-treated β-PIX KD HaCaT, ML-7-treated β-PIX KD HaCaT and β-PIX KD HaCaT cells expressing siRNA targeting MYLK. In B,C, a minimum of eight assays were undertaken in three independent studies. (D) Quantification of the displacement of the wound edge at 12 h after scratching of the indicated monolayers (*n*=3 independent assays with a minimum of four measurements per wound). Bar graphs show means±s.e.m. **P*<0.05, ***P*<0.01, *** *P*<0.001 (Student's *t*-test).

Journal of Cell Science (2017) 130, 2329-2343 doi:10.1242/jcs.196147

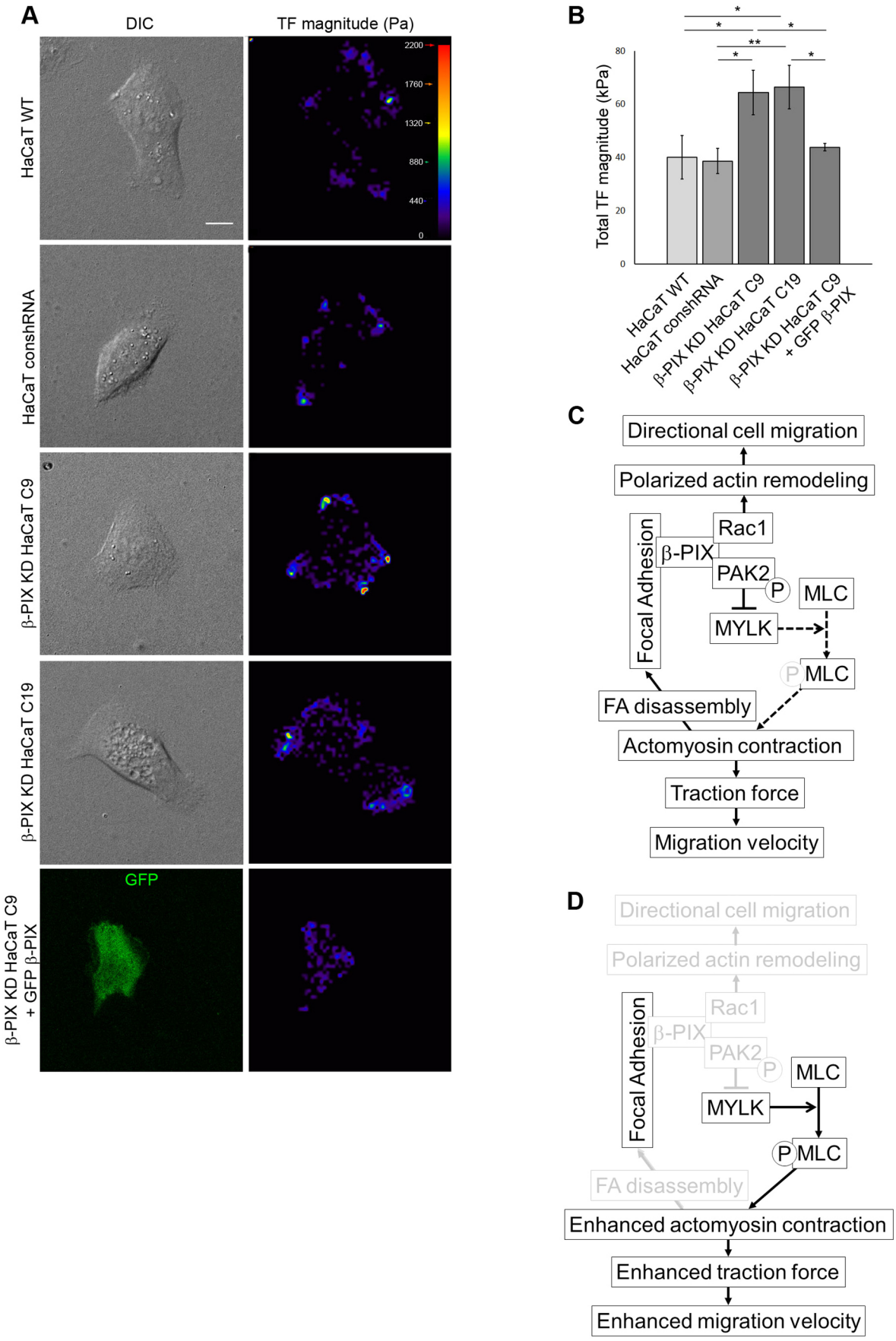

Fig. 8. See next page for legend.

Journal of Cell Science (2017) 130, 2329-2343 doi:10.1242/jcs.196147

Fig. 8. Traction force magnitude in β-PIX KD HaCaT cells and model for role of β-PIX in keratinocytes. (A) Heat maps depicting traction forces greater than 150 Pa in parental HaCaT cells (HaCaT WT), HaCaT cells expressing control shRNA (HaCaT conshRNA), β-PIX KD HaCaT C9 cells, β-PIX KD HaCaT C19 cells and β-PIX KD HaCaT C9+GFP β-PIX cells. The colored bar indicates traction force magnitudes in Pa. Scale bar: 10 µm. (B) Quantification of traction force magnitude in a minimum of 20 cells for each cell population shown in A. Values are means±s.e.m. **P*<0.05, ***P*<0.01 (Student's *t*-test). (C) In wild-type keratinocytes undergoing wound healing, β-PIX localizes to FAs and recruits Rac1 and PAK2. Rac1 regulates directional migration. pPAK2 suppresses MYLK activation and, as a result, phosphorylation of MLC. Decreased pMLC results in a reduction in traction force generation and migration velocity, while facilitating FA disassembly. (D) When β-PIX is knocked down, Rac1 and PAK2 fail to localize to FA. Rac1 mislocalization impairs directional migration. The absence of pPAK2 at FAs causes MYLK activation, and therefore, an increase in pMLC and actomyosin fiber contraction. This enhances traction force and migration velocity, as well as inhibiting FA disassembly.

immunocytochemistry using antibodies against activated Rac1, but unfortunately without success. Regardless, we suggest that loss of β-PIX is likely to result in Rac1 mislocalization in keratinocytes since FAs and hemidesmosome protein complexes, both known to be Rac1 recruitment sites, show aberrant distributions as a consequence of β-PIX knockdown (Sehgal et al., 2006; Chang et al., 2007; Hamill et al., 2009; Hopkinson et al., 2014). Moreover, the potential importance of β-PIX in localizing Rac1 in keratinocytes is indicated by the inability of a SH3-mutant β-PIX to rescue processivity of keratinocytes exhibiting a loss in endogenous β-PIX since the SH3 mutant has been shown to be incapable of binding Rac1, in addition to PAK2 (Manser et al., 1998; ten Klooster et al., 2006).

One curious finding in our studies is that the speed of keratinocytes deficient in β-PIX actually increases. This was an unexpected result since in other cell types studied to date β-PIX loss results in a decrease in cell speed (Nola et al., 2008; Omelchenko et al., 2014; Yu et al., 2015). However, we also present evidence that knockdown of β-PIX increases the forces exerted by keratinocytes on their substrates. Moreover, the knockdown cells also possess larger FAs than control cells and, in the context of collective cell migration, knockdown in follower cells possess many more FAs than their wild-type counterparts. Others have reported that keratinocytes which assemble larger FAs exhibit impaired motility so one might assume that the larger and more numerous FAs in β-PIX KD cells might slow cells (Schober et al., 2007). However, in this regard, recent data have provided evidence that an increase in FA size correlates with increased speed until 'an optimum is reached' (Kim and Wirtz, 2013). Thus, we suggest that the increase in FA size in knockdown cells, together with both the larger numbers of FAs and traction forces they exert, might explain their enhanced speed of the knockdown cells compared to controls. Indeed, both the size and density of FA in each area, especially the size in the LF, are correlated with the cell speed during collective cell migration (Fig. S5). However, in this regard, we also show that FA size is reduced in β-PIX KD cells following inhibition of ROCK proteins and yet the treated cells move faster. Thus, we propose that both FA size and the ability of FAs to transduce signals are important regulators of cell motility, depending on context.

Our data regarding β-PIX functions in keratinocytes lead to a conundrum. Why is a negative regulator of motility (in this case β-PIX) actively recruited to FAs at the leading edge of sheets of keratinocytes undergoing wound healing *in vitro*? Despite this apparent contradiction, there is a precedent for our finding. It has been reported that the small GTPase regulator ARHGAP4 is recruited to the leading front of 3T3 cells where it inhibits their motility (Vogt et al., 2007). Thus, β-PIX in keratinocytes and ARHGAP4 in 3T3 cells may act as brakes to cell movement. We propose that β-PIX does so by localizing PAK2 to FAs, thereby fine tuning MYLK-regulated actomyosin contractility, traction force generation and FA turnover in leader cells (depicted in Fig. 8C). In contrast, β-PIX loss inhibits recruitment of PAK2 to FAs, which, in turn, induces a localized promotion of the activity of MYLK (Fig. 8D). In other words, in β-PIX KD cells, MYLK is active at or close by FAs. This facilitates an increase in phosphorylation of MLC and enhanced contraction of the actomyosin cytoskeleton, which inhibits the disassembly of FAs. Enhanced actomyosin contraction causes an augmentation in traction forces exerted by the KD cells on their substrate (Fig. 8D). Overall, this leads to an increase in speed of KD cells compared to their control counterparts. Thus, unexpectedly, our data suggest the intriguing possibility that epithelialization of a healing wound of the skin can be accelerated by either decreasing β-PIX expression or, potentially, by inhibiting its functions locally at a wound site.

MATERIALS AND METHODS

Cell culture, lentiviral infection, and transfection protocols and drug treatments

HaCaT cells were cultured in Dulbecco's modified Eagle's medium (DMEM; HyClone, Logan, UT) supplemented with 10% fetal bovine serum (Sigma-Aldrich, St. Louis, MO) and 1% penicillin-streptomycin mixture at 37°C (Thermo Fisher Scientific, Waltham, MA). These cells were obtained originally from Dr Norbert Fusenig (Heidelberg, Germany) in the 1990s. Their human keratinocyte nature is routinely confirmed by RT-PCR and reactivity with antibodies specific human keratinocyte proteins, including the bullous pemphigoid antigens and β4 integrin. N/TERT cells were cultured in DMEM supplemented with 25% of the DMEM nutrient mixture Ham's F-12 (Sigma-Aldrich), 10% fetal bovine serum, 1% penicillin-streptomycin, 10 ng ml^{-1} epidermal growth factor, 0.4 µg ml^{-1} hydrocortisone, 5 µg ml^{-1} insulin, and 8.67 ng ml^{-1} cholera toxin mixture at 37°C. These cells were a generous gift from Kristin Braun (Centre for Cutaneous Research, Blizard Institute, Barts and The London School of Medicine and Dentistry, London, UK). β-PIX KD HaCaT and N/TERT cells were generated by using ARHGEF7 MISSION shRNA lentiviral transduction particles TRCN0000047596 (Sigma-Aldrich) (Table S1). HaCaT cells expressing control shRNA were established with same procedure by using MISSION pLKO.1-puro Non-Target shRNA Control Plasmid DNA (Table S1). In brief, cells were seeded into six-well plates overnight, then infected with the lentivirus encoding β-PIX or control shRNA at a multiplicity of infection (MOI) of 0.5 in culture medium supplemented with polybrene (8 µg ml^{-1}; Thermo Fisher Scientific). The next day, the medium was replaced with puromycin-containing medium (0.5 µg ml^{-1}), and the surviving cells cloned by serial dilution. β-PIX protein levels in the resulting clones were evaluated by immunoblotting.

To induce the expression of GFP-tagged β-PIX, GFP-tagged β-PIX mutants or GFP-tagged paxillin, cells were passaged a day before transfection. Plasmid vectors encoding the tagged proteins were transfected into the cells by using Lipofectamin 3000 with Opti-MEM (Thermo Fisher Scientific) following the manufacturer's protocol. Cells transfected with GFP-tagged paxillin were analyzed 18–30 h after the transfection. Populations of GFP-tagged β-PIX and GFP-tagged β-PIX mutant transfectants were processed for FACS using a Sony SH800 cell sorter (Sony Biotechnology Inc., San Jose, CA), according to GFP intensity at 18–30 h after transfection. Sorted cells were analyzed by western blotting, staining or through a motility assay at 18–30 h after the sorting. To induce MYLK KD, cells were transfected with 100 nM of siRNA targeting MYLK (NM_053025, SASI_Hs01_00194703; Sigma-Aldrich) using Lipofectamin 3000 and Opti-MEM. After 36 h, cells were used for experiments.

For inhibition studies, 50 µM MYLK inhibitor ML-7 (Sigma-Aldrich), 10 mM myosin II inhibitor blebbistatin (Millipore, Darmstadt, Germany), 5 µM of ROCK inhibitor Y-27632 (Sigma-Aldrich) or vehicle (DMSO,

Journal of Cell Science (2017) 130, 2329-2343 doi:10.1242/jcs.196147

Sigma-Aldrich) were added to cultures. For immunostaining analysis, these drugs were added 3 h after scratch wounding, and incubated for 1 h prior to analyses. For the motility assay, the drugs were added immediately after the scratch wounding and cells were incubated with the drugs during the assay.

Antibodies and fluorescence probes

Mouse monoclonal antibody against talin (8d4) was purchased from Sigma-Aldrich. A rabbit monoclonal antibodies against paxillin (Y113), PAK2 (EP796Y), and myosin light chain 2 (EPR3741) were purchased from Abcam (Cambridge, MA). Rabbit monoclonal antibody against GFP (G10362) and Rhodamine- or Alexa Fluor 647-conjugated phalloidin were purchased from Thermo Fisher Scientific. Rabbit polyclonal antibody against the β-PIX SH3 domain (07-1450) and mouse monoclonal antibody against glyceraldehyde-3-phosphate dehydrogenase (GAPDH; MAB374) were purchased from Millipore. Polyclonal antibodies against lamin A/C and phospho-myosin light chain 2 (Ser19) (#3671) were purchased from Cell Signaling Technology (Danvers, MA). A mouse monoclonal antibody against β4 integrin (CD104) (450-9D) was purchased from BD Biosciences (San Jose, CA). Alexa Fluor 488- or Alexa Fluor 647-conjugated goat anti-mouse-IgG and Alexa Fluor 488- or Alexa Fluor 647-conjugated goat anti-rabbit-IgG were purchased from Thermo Fisher Scientific. Primary and secondary antibodies are used at 1:100 and 1:500 dilution, respectively, for immunolocalization studies and at 1:1000 for immunoblotting studies. They were validated by testing on knockdown lines or by undertaking combination immunoblotting/immunofluorescence studies on lines in which the expression and localization of the antigen under assay are well established.

Immunofluorescence analyses

Cells on glass coverslips were processed for staining as detailed elsewhere (Klatte et al., 1989). In brief, cells were fixed with 3.7% formaldehyde (Thermo Fisher Scientific) for 10 min and permeabilized with 0.5% Triton X-100 (Sigma-Aldrich) at 4°C for 10 min followed by incubations with primary and secondary antibodies at 37°C for 1 h each. All samples were observed with a Leica TCS SP5 confocal or TCS SP8 X confocal microscope (Leica Microsystems, Buffalo Grove, IL). Images were exported as TIFF files and processed using ImageJ (National Institutes of Health, Bethesda, MD). Figures were prepared using Adobe Photoshop (Adobe Systems, San Jose, CA).

Quantification of FA size, FA density and generation of intensity ratios of FA antibody staining

Cells were plated onto the coverslip 18 h prior to the scratch wounding. The confluent cells were scratched and fresh medium was added to the cultures. After 4 h incubation, cells were fixed and stained with anti-paxillin and/or anti-talin antibodies. All images, except for the images of HaCaT cells in Fig. 1B and of β-PIX KD HaCaT cells expressing wild-type or mutant β-PIX in Fig. 4F,G, were unlabeled and analyzed blind. Using ImageJ, background signals in the cytoplasm were subtracted (Fig. S6A). With the wand tool, each FA was outlined and their number and size were quantified (Fig. S6A,B). FA size measurements were logarithmically transformed in order to fit the data to a normal distribution. FA density was determined by assaying the numbers of FA per defined area of the LF or DZ. To generate ratios of the staining intensity of FA antibody pairs, background staining was first subtracted and then the intensities of staining of each pair in FAs was measured by using the wand tool.

SDS-PAGE, western blotting and RT-qPCR analyses

Whole-cell extracts were prepared and then processed for SDS-PAGE and western blot analysis as previously described (Harlow and Lane, 1988). The Thermo Scientific Page Ruler Plus Prestained Protein Ladder provided standards for molecular mass determination. Western blots were visualized by using a myECL Imager (Thermo Fisher Scientific) and then quantified with ImageJ. For immunoblotting of pMLC and MLC, the antibody against pMLC was stripped and the membrane was reproved with MLC antibody.

Total RNA was extracted from cells using a GeneJET RNA Purification Kit (Thermo Fisher Scientific). 5 ng of extracted RNA was used to synthesize cDNA using a Maxima H Minus First Strand cDNA Synthesis Kit with dsDNase (Thermo Fisher Scientific). mRNA expression was analyzed using a Step One Plus Real-Time PCR System (Thermo Fisher Scientific) with TaqMan Fast Advanced Master Mix and TaqMan Gene Expression Assays (Thermo Fisher Scientific) for MYLK (Hs00364926_m1) and GAPDH (Hs02758991_g1). Relative gene expression was quantified by a ΔΔCt method and normalized to the expression of *GAPDH*.

Single-cell motility and scratch wound assay

For the single-cell motility assay, cells were plated onto substrates coated with laminin-332-rich 804G cell conditioned medium 4 h before the assay. Cells were imaged every 10 min over 3 h using a Leica DMi8 microscope, and cell motility behavior was analyzed using MetaMorph software (MolecularDevices, Sunnyvale, CA). For each cell type, speed and processivity were calculated. Processivity was defined as the maximum displacement from the origin of the cell divided by the path length.

For the single-cell motility assay on the gel, polyacrylamide gels were prepared as previously described to generate substrates with a stiffness of ∼12 kPa and 51 kPa (Eisenberg et al., 2011). The gels were activated with sulfo-SANPAH (Thermo Fisher Scientific) and coated with laminin-332-rich 804G cell conditioned medium. Cells were plated onto the gels 18 to 24 h before the assay. Cells were imaged and analyzed with same procedures for the single-cell motility assay on the cell culture dish.

For the scratch wound assay, confluent cells on 12-well plates were scratched with a pipette tip. Immediately after wounding, the cultures were fed with fresh medium supplemented with 50 mM 4-(2-hydroxyethyl)-1-piperazineethanesulfonic acid (HEPES) (Sigma-Aldrich) and observed in a heated chamber at 37°C. Images were taken every 5 min over 12 h with the Leica DMi8 microscope. The average displacement of the leading edge of the cell sheet was calculated at 6 and 12 h after the scratch with ImageJ.

Construct generation

To generate the GFP-tagged β-PIX construct, total RNA was extracted from 804G cells using the GeneJet RNA purification kit and reverse transcribed into cDNA (Maxima H Minus First Strand cDNA Synthesis Kit with dsDNase). A full length β-PIX coding sequence was generated from the cDNA by PCR using primers foward, 5′-AATTAGATCTATGACTGATA-ACGCC AACAGCCAACTG-3′ and reverse, 5′-TTAAGAATTCCTATAG-ATTGGTCTCATCCCAAGCAG-3′. The β-PIX PCR product was digested and cloned in-frame into pEGFPC (Takara Bio USA, Inc., Mountain View, CA) and sequenced completely. A mammalian expression plasmid containing the complete coding sequence of chicken paxillin fused to GFP was a gift from Dr Milan Mrksich, Northwestern University, Chicago, IL.

To generate the GFP-tagged SH3 mutant (W43P and W44G) or GEF-deficient (L238R and L239S) β-PIX constructs, the GFP-tagged β-PIX construct was mutated with the QuikChange Lightning site-directed mutagenesis kit (Agilent Technologies, Santa Clara, CA) following the manufacturer's protocol. The mutations were confirmed by DNA sequencing.

Quantification of FA assembly and disassembly

Confluent HaCaT cells maintained on glass-bottomed dishes (MatTek, Ashland, MA) were transfected with a construct encoding GFP-tagged paxillin. At 18–30 h after transfection, the monolayer cell sheets were scratch wounded, and the medium was changed to Phenol Red-free serum-containing DMEM (HyClone, Logan, UT) supplemented with OxyFluor (Oxyrase, West Mansfield, OH) and 50 mM HEPES. At 1 h after the scratch, FAs at both the LF and DZ were imaged with the Leica DMi8 microscope with the heated chamber at 37°C. Images were taken every 5 min for 4 h. The images were analyzed to quantify the GFP intensity with ImageJ. The mean intensity of GFP at the FA, with the intensity of GFP around the FA subtracted in each time frame, was used to determine FA assembly and disassembly rate as described elsewhere (Stehbens and Wittmann, 2014).

Rac1 activation assay

Cells were plated on the dish and incubated for 18 to 24 h. Confluent cells were scratch wounded 4 h before the assay. Rac1 activation was quantified

using a G-LISA assay kit (Cytoskeleton, Inc., Denver, CO) according to the manufacturer's protocol.

Traction force microscopy

Traction force microscopy was performed as described elsewhere (Eisenberg et al., 2013; Hiroyasu et al., 2016). In brief, cells were plated on polyacrylamide gels embedded with fluorescent beads. After taking images of live cells and beads using the Leica TCS SP8 X microscope, cells were detached through treatment with trypsin and then an image of beads taken. The bead displacement was used to calculate traction forces by using the StackReg, Iterative Particle Image Velocimetry and FTTC plugins for ImageJ following protocols detailed by others (Tseng et al., 2012).

Correlation analysis

To assess the relationship of FA size and density to cell speed in collective cell migration in different cell types, each mean value of the FA size in LF, FA size in DZ, FA density in LF, FA density in DZ, and the displacement of the wound edge were normalized by subtracting the minimum value and dividing by the range of the mean values (Fig. S5). The maximum and minimum values in each cell type (HaCaT or N/TERT cells) were designated as 1 and 0, respectively, and all other data ranged between 0 to 1. Normalized data were analyzed using a linear regression model.

Statistics

All experiments were performed a minimum of three times and analyzed with R software (R Foundation for Statistical Computing, Vienna, Austria). Statistical significance was determined by Student's *t*-test for all data, and is indicated by a bar and asterisk above each data set. A value of $P<0.05$ was considered significant. Where no significance was detected, no bar is included in the figures.

Acknowledgements

We thank Melissa Oatley of SMB for her assistance with FACS analyses.

Competing interests

The authors declare no competing or financial interests.

Author contributions

Conceptualization: J.C.R.J.; Methodology: S.H., G.P.S., S.B.H., J.C.R.J.; Validation: J.C.R.J.; Formal analysis: S.H., G.P.S., S.B.H., J.C.R.J.; Resources: S.B.H.; Writing - original draft: S.H., J.C.R.J.; Writing - review & editing: S.H., J.C.R.J.; Visualization: S.H.; Supervision: J.C.R.J.

Funding

Research reported in this publication was supported by the National Institute of Arthritis and Musculoskeletal and Skin Diseases of the National Institutes of Health (award number R01 AR054184 to J.C.R.J.). The content is solely the responsibility of the authors and does not necessarily represent the official views of the National Institutes of Health. Deposited in PMC for release after 12 months.

Supplementary information

Supplementary information available online at
http://jcs.biologists.org/lookup/doi/10.1242/jcs.196147.supplemental

References

Audebert, S., Navarro, C., Nourry, C., Chasserot-Golaz, S., Lécine, P., Bellaiche, Y., Dupont, J.-L., Premont, R. T., Sempéré, C., Strub, J.-M. et al. (2004). Mammalian scribble forms a tight complex with the βPIX exchange factor. *Curr. Biol.* **14**, 987-995.

Burnette, D. T., Manley, S., Sengupta, P., Sougrat, R., Davidson, M. W., Kachar, B. and Lippincott-Schwartz, J. (2011). A role for actin arcs in the leading-edge advance of migrating cells. *Nat. Cell Biol.* **13**, 371-382.

Cau, J. and Hall, A. (2005). Cdc42 controls the polarity of the actin and microtubule cytoskeletons through two distinct signal transduction pathways. *J. Cell Sci.* **118**, 2579-2587.

Chang, F., Lemmon, C. A., Park, D., Lewis, H. and Romer, L. H. (2007). FAK potentiates Rac1 activation and localization to matrix adhesion sites: a role for βPIX. *Mol. Biol. Cell* **18**, 253-264.

Chew, T.-L., Masaracchia, R. A., Goeckeler, Z. M. and Wysolmerski, R. B. (1998). Phosphorylation of non-muscle myosin II regulatory light chain by p21-activated kinase (gamma-PAK). *J. Muscle Res. Cell Motil.* **19**, 839-854.

Dickson, M. A., Hahn, W. C., Ino, Y., Ronfard, V., Wu, J. Y., Weinberg, R. A., Louis, D. N., Li, F. P. and Rheinwald, J. G. (2000). Human keratinocytes that express hTERT and also bypass a p16(INK4a)-enforced mechanism that limits life span become immortal yet retain normal growth and differentiation characteristics. *Mol. Cell. Biol.* **20**, 1436-1447.

Eisenberg, J. L., Safi, A., Wei, X., Espinosa, H. D., Budinger, G. S., Takawira, D., Hopkinson, S. B. and Jones, J. C. (2011). Substrate stiffness regulates extracellular matrix deposition by alveolar epithelial cells. *Res. Rep. Biol.* **2011**, 1-12.

Eisenberg, J. L., Beaumont, K. G., Takawira, D., Hopkinson, S. B., Mrksich, M., Budinger, G. R. S. and Jones, J. C. R. (2013). Plectin-containing, centrally localized focal adhesions exert traction forces in primary lung epithelial cells. *J. Cell Sci.* **126**, 3746-3755.

Gallegos, L., Ng, M. R. and Brugge, J. S. (2011). The myosin-II-responsive focal adhesion proteome: a tour de force? *Nat. Cell Biol.* **13**, 344-346.

Goeckeler, Z. M., Masaracchia, R. A., Zeng, Q., Chew, T.-L., Gallagher, P. and Wysolmerski, R. B. (2000). Phosphorylation of myosin light chain kinase by p21-activated Kinase PAK2. *J. Biol. Chem.* **275**, 18366-18374.

Hamill, K. J., Hopkinson, S. B., DeBiase, P. and Jones, J. C. R. (2009). BPAG1e maintains keratinocyte polarity through beta4 integrin-mediated modulation of Rac1 and cofilin activities. *Mol. Biol. Cell* **20**, 2954-2962.

Harlow, E. and Lane, D. (1988). In laboratory. In *Antibodies: A Laboratory Manual* (ed. C. S. H.), pp. 92-121. New York: Cold Spring Harbor.

Hiroyasu, S., Colburn, Z. T. and Jones, J. C. R. (2016). A hemidesmosomal protein regulates actin dynamics and traction forces in motile keratinocytes. *FASEB J.* **30**, 2298-2310.

Hopkinson, S. B., Hamill, K. J., Wu, Y., Eisenberg, J. L., Hiroyasu, S. and Jones, J. C. R. (2014). Focal contact and hemidesmosomal proteins in keratinocyte migration and wound repair. *Adv. Wound Care* **3**, 247-263.

Jackson, B., Peyrollier, K., Pedersen, E., Basse, A., Karlsson, R., Wang, Z., Lefever, T., Ochsenbein, A. M., Schmidt, G., Aktories, K. et al. (2011). RhoA is dispensable for skin development, but crucial for contraction and directed migration of keratinocytes. *Mol. Biol. Cell* **22**, 593-605.

Kim, D.-H. and Wirtz, D. (2013). Focal adhesion size uniquely predicts cell migration. *FASEB J.* **27**, 1351-1361.

Kiosses, W. B., Daniels, R. H., Otey, C., Bokoch, G. M. and Schwartz, M. A. (1999). A role for p21-activated kinase in endothelial cell migration. *J. Cell Biol.* **147**, 831-844.

Klatte, D. H., Kurpakus, M. A., Grelling, K. A. and Jones, J. C. R. (1989). Immunochemical characterization of three components of the hemidesmosome and their expression in cultured epithelial cells. *J. Cell Biol.* **109**, 3377-3390.

Kuo, J.-C., Han, X., Hsiao, C.-T., Yates, J. R., III and Waterman, C. M. (2011). Analysis of the myosin-II-responsive focal adhesion proteome reveals a role for β-Pix in negative regulation of focal adhesion maturation. *Nat. Cell Biol.* **13**, 383-393.

Manser, E., Loo, T.-H., Koh, C.-G., Zhao, Z.-S., Chen, X.-Q., Tan, L., Tan, I., Leung, T. and Lim, L. (1998). PAK kinases are directly coupled to the PIX family of nucleotide exchange factors. *Mol. Cell* **1**, 183-192.

Nola, S., Sebbagh, M., Marchetto, S., Osmani, N., Nourry, C., Audebert, S., Navarro, C., Rachel, R., Montcouquiol, M., Sans, N. et al. (2008). Scrib regulates PAK activity during the cell migration process. *Hum. Mol. Gen.* **17**, 3552-3565.

Oakes, P. W. and Gardel, M. L. (2014). Stressing the limits of focal adhesion mechanosensitivity. *Curr. Opin. Cell Biol.* **30**, 68-73.

Omelchenko, T., Rabadan, M. A., Hernández-Martínez, R., Grego-Bessa, J., Anderson, K. V. and Hall, A. (2014). β-Pix directs collective migration of anterior visceral endoderm cells in the early mouse embryo. *Genes Dev.* **28**, 2764-2777.

Sanders, L. C., Matsumura, F., Bokoch, G. M. and de Lanerolle, P. (1999). Inhibition of myosin light chain kinase by p21-activated kinase. *Science* **283**, 2083-2085.

Santiago-Medina, M., Gregus, K. A. and Gomez, T. M. (2013). PAK–PIX interactions regulate adhesion dynamics and membrane protrusion to control neurite outgrowth. *J. Cell Sci.* **126**, 1122-1133.

Schober, M., Raghavan, S., Nikolova, M., Polak, L., Pasolli, H. A., Beggs, H. E., Reichardt, L. F. and Fuchs, E. (2007). Focal adhesion kinase modulates tension signaling to control actin and focal adhesion dynamics. *J. Cell Biol.* **176**, 667-680.

Sehgal, B. U., DeBiase, P. J., Matzno, S., Chew, T.-L., Claiborne, J. N., Hopkinson, S. B., Russell, A., Marinkovich, M. P. and Jones, J. C. R. (2006). Integrin beta4 regulates migratory behavior of keratinocytes by determining laminin-332 organization. *J. Biol. Chem.* **281**, 35487-35498.

Sells, M. A., Boyd, J. T. and Chernoff, J. (1999). p21-Activated Kinase 1 (Pak1) regulates cell motility in mammalian fibroblasts. *J. Cell Biol.* **145**, 837-849.

Stehbens, S. J. and Wittmann, T. (2014). Analysis of focal adhesion turnover: a quantitative live-cell imaging example. *Methods Cell Biol.* **123**, 335-346.

Stehbens, S. J., Paszek, M., Pemble, H., Ettinger, A., Gierke, S. and Wittmann, T. (2014). CLASPs link focal-adhesion-associated microtubule capture to localized exocytosis and adhesion site turnover. *Nat. Cell Biol.* **16**, 561-573.

ten Klooster, J. P., Jaffer, Z. M., Chernoff, J. and Hordijk, P. L. (2006). Targeting and activation of Rac1 are mediated by the exchange factor β-Pix. *J. Cell Biol.* **172**, 759-769.

Tseng, Q., Duchemin-Pelletier, E., Deshiere, A., Balland, M., Guillou, H., Filhol, O. and Théry, M. (2012). Spatial organization of the extracellular matrix regulates cell-cell junction positioning. *Proc. Natl. Acad. Sci. USA* **109**, 1506-1511.

Turner, C. E., Brown, M. C., Perrotta, J. A., Riedy, M. C., Nikolopoulos, S. N., McDonald, A. R., Bagrodia, S., Thomas, S. and Leventhal, P. S. (1999). Paxillin LD4 motif binds PAK and PIX through a novel 95-kD ankyrin repeat, ARF-GAP protein: a role in cytoskeletal remodeling. *J. Cell Biol.* **145**, 851-863.

Vogt, D. L., Gray, C. D., Young, W. S., III, Orellana, S. A. and Malouf, A. T. (2007). ARHGAP4 is a novel RhoGAP that mediates inhibition of cell motility and axon outgrowth. *Mol. Cell. Neuro.* **36**, 332-342.

Wolfenson, H., Bershadsky, A., Henis, Y. I. and Geiger, B. (2011). Actomyosin-generated tension controls the molecular kinetics of focal adhesions. *J. Cell Sci.* **124**, 1425-1432.

Yu, H. W., Chen, Y.-Q., Huang, C.-M., Liu, C.-Y., Chiou, A., Wang, Y.-K., Tang, M.-J. and Kuo, J.-C. (2015). β-PIX controls intracellular viscoelasticity to regulate lung cancer cell migration. *J. Cell. Mol. Med.* **19**, 934-947.

Zhao, X. and Guan, J.-L. (2011). Focal adhesion kinase and its signaling pathways in cell migration and angiogenesis. *Adv. Drug Del. Rev.* **63**, 610-615.

Zhao, Z.-S., Manser, E., Loo, T.-H. and Lim, L. (2000). Coupling of PAK-interacting exchange factor PIX to GIT1 promotes focal complex disassembly. *Mol. Cell. Biol.* **20**, 6354-6363.